PHYSICAL REVIEW B **78**, 121404(R) (2008)

Dynamic structure in supported Pt nanoclusters: Real-time density functional theory and x-ray spectroscopy simulations

F. Vila,[1] J. J. Rehr,[1,*] J. Kas,[1] R. G. Nuzzo,[2] and A. I. Frenkel[3]
[1]*Department of Physics, University of Washington, Seattle, Washington 98195, USA*
[2]*Department of Chemistry, University of Illinois at Urbana-Champaign, Urbana, Illinois 61801, USA*
[3]*Department of Physics, Yeshiva University, New York, New York 10016, USA*

(Received 24 July 2008; published 11 September 2008)

The nature of local atomic and electronic structure at the nanoscale is of both fundamental and technological importance. For example, supported metal nanoclusters exhibit a number of unusual phenomena including large structural disorder and bond-length contraction with increasing temperature. We investigate this behavior for a prototypical ten atom Pt cluster supported on γ alumina using temperature-dependent, real-time simulations based on density functional theory/molecular-dynamics and x-ray spectroscopy theory. The simulations reveal a complex dynamical structure on multiple-time scales including librational motion of the center of mass and fluctuating bonding characteristics, which explain many of the unusual properties.

DOI: 10.1103/PhysRevB.78.121404 PACS number(s): 61.05.cj, 71.15.Pd, 65.80.+n, 71.15.Mb

The physics and chemistry of nanoscale systems are of considerable fundamental and technological importance. Oxide supported metal nanoclusters constitute an important class of such systems, with unique catalytic properties.[1] However, the relationship between their structural and electronic properties as well as their influence on catalysis remains largely unresolved. Indeed, the intrinsic complexity of these systems has generated both attention and controversy for years.[2–4] Evidently such systems have unusual physical properties, as observed in recent x-ray absorption spectroscopy experiments.[5] For example, Pt nanoclusters on γ alumina were found to exhibit large disorder, bond-length contraction with increasing temperature [i.e., negative thermal bond-length expansion (NTE)] and thermally induced changes in electronic structure. A major difficulty in understanding these effects is that traditional methods of theory and analysis designed for bulk structures tend to be ill suited for studying nanoscale behavior. Thus different modeling techniques are called for,[6] e.g., based on a combination of theory and experiment.[7] As an example of such a combined approach, we present temperature-dependent density functional theory/molecular-dynamics (DFT/MD) calculations[8,9] of the simulated real-time behavior of supported Pt nanoclusters on [110] γ alumina together with calculations of their x-ray absorption spectra (XAS). These simulations reveal a rich dynamical structure over multiple time scales, ranging from internal vibrations and flexing modes to stochastic librational and transient motion of the center of mass. The physical picture revealed by our DFT/MD simulations is that of a flexible nanocluster tethered to the surface by a few transient surface bonds. These characteristics are key to unraveling many of the unusual properties of these systems. To illustrate this behavior, time-elapsed renderings of the structure for the low (165 K) and high (573 K) temperatures of the experiment[5] are shown in Fig. 1. Further details are given in the supplementary material.[10]

DFT/MD simulations are advantageous for understanding the dynamics of such complex systems since they naturally sample relevant configurations with appropriate Boltzmann statistics. It is useful to analyze the dynamics of these systems in terms of center of mass (CM) and internal motion. While large CM fluctuations are ultimately responsible for many of the unusual properties of these systems, x-ray spectra depend primarily on their internal structure. The librational motion of the CM is thermally driven and reflects a hindered Brownian motion in two dimensions. Thus diffusive motion is generally constrained by Pt-O bonds at the surface. However, due to the transient behavior of the Pt-O bonds that occasionally break and reform, transient displacements are sometimes observed. The librational fluctuations[10] are of angstrom amplitude, i.e., an order of magnitude larger than typical vibrations, and are accompanied by CM speeds $v \approx 0.7\ \text{Å/ps} \approx 70\ \text{m/s}$. This is consistent with the equipartition theorem result for the rms speed $v = \sqrt{2k_BT/M}$, where M is the cluster mass and k_B is Boltzmann's constant. Thus such motion is expected to be generally important for tethered clusters at the nanoscale when M is sufficiently small. Although librational motion has also been investigated in the surface dynamics of small molecular systems,[11,12] its role in nanostructure dynamics has been heretofore unexplored. Increased fluctuations in cluster surface atoms have also been found in other recent experiments.[13]

Our DFT/MD simulations were carried out for a prototypical Pt_{10} nanocluster on the "*d*" layer of the [110] surface of γ-Al_2O_3 using the VASP code optimized for MD simulations,[14] starting from an initial ground-state structure and cluster position. To check the possible dependence of the results on the starting point, we repeated the DFT/MD calculations for two additional cluster starting configurations. Remarkably, despite noticeable differences in the stochastic CM motion, the simulations all gave closely similar results for the ensemble of internal structures. Subsequently a configurationally averaged XAS was calculated using a parallel version of the real-space multiple-scattering code FEFF8.2,[15,16] which is well suited for Pt XAS studies.[17] The DFT calculations used a standard Perdew-Burke-Ernzerhof (PBE) exchange-correlation functional[18] with a plane-wave cut-off energy of 396 eV, and were performed using the DOE NERSC high-performance computer facility. The MD included a Nose thermostat and a time step of 3 fs, which is

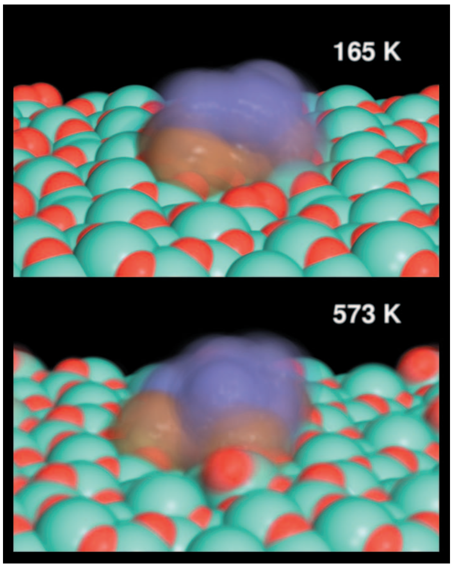

FIG. 1. (Color) Time-elapsed rendering of the structure of a Pt_{10} cluster on [110] γ-Al_2O_3. The purple and gold spheres represent Pt atoms that are metallic and oxidized, respectively, with the latter being bound to surface O atoms, while the red and turquoise spheres represent oxygen and aluminum atoms, respectively. The “blurriness” of a given atom characterizes its range of motion.

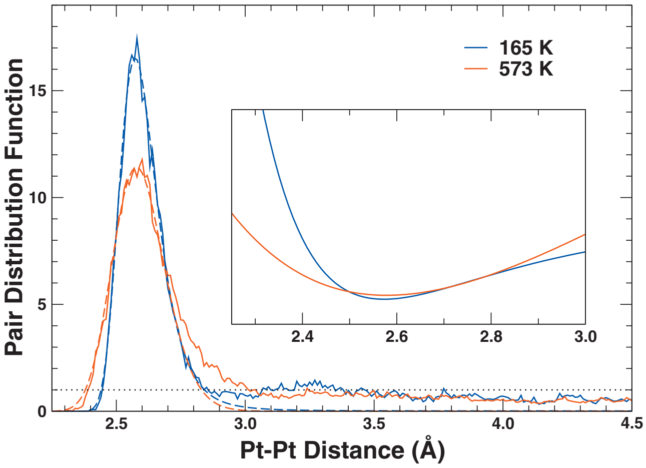

FIG. 2. (Color) Pt-Pt pair distribution function and fits (dashed lines) to asymmetric 1nn distributions $g(r)$ generated by *ad hoc* Morse potentials (see text). The inset shows the effective Pt-Pt pair potentials that characterize the thermal and structural disorders at 165 (blue) and 573 K (red).

small enough to capture even the short-time vibrational motion. After a period of ≈ 3 ps, which is adequate to achieve thermal equilibrium, the calculations were continued for another 5.5 ps to sample the phase space including several librational periods. The DFT/MD calculations for these systems are computationally intensive, and altogether required about 2×10^4 cpu h. Hence they could only be done in a reasonable time on modern high-performance machines. Considerably more time would be needed to simulate the full Pt cluster size distribution including the bonding of adsorbates such as H or the long-time diffusive motion. However, separate DFT calculations were carried out to show that the inclusion of cluster-bound H atoms weakens the Pt-Pt bonds, leading to an increase in the Pt-Pt bond length consistent with experimental observations. Although some previous DFT/MD supported-cluster simulations have been carried out,[19] they were applied to carbon-supported nanoclusters not displaying the electronic or structural anomalies discussed here.

We find that the results for our prototypical Pt_{10} cluster already give a qualitative explanation of the unusual behavior of these systems. The configurations generated by the DFT/MD time series can be characterized by the pair distribution function (PDF) $g(r)$ and its moments. To be consistent with extended x-ray absorption fine structure (EXAFS) analysis,[5] we evaluate the mean Pt-Pt distance in terms of the first nearest-neighbor PDF. We find that the asymmetric PDF from our MD time series is well converged and can be parametrized well in terms of an effective, anharmonic pair potential[20] $g(r)=Ae^{-\Phi(r)}$, where Φ is represented by a Morse potential $\Phi(r)=\beta D[e^{-\alpha(r-r_0)}-1]^2$ with temperature-dependent parameters A, D, α, r_0 (Fig. 2, dashed lines). This parametrization allows one to visualize the effective pair potentials (inset of Fig. 2) and simplifies the analysis.[21,22] A factor $\beta=1/k_BT$ is included for convenience, in analogy with model PDFs for vibrational motion. Both the temperature dependence and increased width of Φ at short distances are striking, and differ from conventional vibrational dynamics with constant pair potentials and hard-core repulsion. Table I presents the mean distances R, the mean square relative displacements (MSRD) σ^2 including structural and vibrational disorders, and the mean first neighbor (1nn) coordination numbers N.

Clearly, the change in the mean distances between 165 and 573 K confirms NTE for a Pt_{10} cluster with net decrease of $\Delta R=-0.008$ Å. Although smaller than the experimentally

TABLE I. Average distance R, MSRD σ^2, and mean coordination number N as a function of temperature for the different Pt-Pt and Pt-O bonds (see text) based on Morse-potential PDF parametrizations.

	R (Å)		σ^2 (10^{-3} Å^2)		N	
Bond	165 K	573 K	165 K	573 K	165 K	573 K
Pt-Pt	2.602	2.594	5.2	10.0	3.2	2.9
Pt_O-Pt_O	2.627	2.613	3.5	7.3	0.7	0.4
Pt_M-Pt_M	2.637	2.598	5.4	10.8	1.0	1.0
Pt_O-Pt_M	2.560	2.596	3.3	8.6	1.5	1.5
Pt-O	2.076	2.086	2.2	9.2	0.4	0.6

observed decrease of −0.027 Å, the experimental measurements were carried out for a range of cluster sizes between 5 and 25 Pt atoms rather than a single ten atom cluster. Also the large structural and vibrational disorders given by the simulations (Table I) are in rough agreement with the experimental values[5] for the 5–25 atom distribution, 8×10^{-3} Å^2 (10×10^{-3} Å^2) at low (high) temperature. Finally, the mean coordination numbers N are smaller than the mean experimental value ≈5.5 for the 5–25 atom clusters, as expected for a small cluster.

To understand better the structural changes with temperature and the role played by the surface, we decompose the Pt-Pt PDF into two distinct populations of Pt atoms: namely the subsets that are (i) in contact with O atoms at the surface (Pt_O or *oxidized*) and (ii) those only in contact with other Pt atoms (Pt_M or *metallic*). This decomposition generates three pair distributions: Pt_O-Pt_O, Pt_M-Pt_M, and Pt_O-Pt_M, which help explain some of the unusual properties of these nanoclusters. First, the Pt_O-Pt_O and Pt_M-Pt_M bonds show considerable NTE (−0.014 and −0.039 Å, respectively). For the Pt_{10} cluster this is partly counterbalanced by a 0.036 Å positive thermal expansion for the Pt_O-Pt_M bonds. Second, the average R for bonds between oppositely charged species is smaller than that for similarly charged species. Third, the reduction in N at high temperature is largely due to a decrease in the number of Pt_O-Pt_O bonds. Finally, the weak, broad peaks in the PDF between 3.1–3.4 Å are due largely to Pt_O-Pt_M bonds. This secondary structure is a consequence of the spatial segregation of the metallic and oxidized populations, i.e., the Pt_O and Pt_M atoms tend to lie on distinct, nonoverlapping layers.[10] The physical reason for these differences can be attributed to charge transfer, as shown by electronic structure and XAS calculations described below. The Pt-O bonds play an important role in binding the cluster to a given region of the surface. Our simulations reveal wide Pt-O bond-length distributions that differ among the O atoms attached to the cluster. The difficulty of observing the O atoms in XAS is likely due to the wide Pt-O distributions and the weakness of O scattering. Interestingly, while the Pt cluster at low temperature sees a somewhat structured support with peaks in the PDF above 3 Å, this structure is washed out at high temperature and the support is seen as homogeneous.[10] Overall, it appears that the mechanism responsible for the observed NTE is largely due to the librational motion, which leads to increased disorder at high temperatures, rather analogous to that for entropy-driven transitions between solid and disordered phases, e.g., in H_2O.[23]

We now turn to the analysis of the XAS, which is often used for structural investigations of nanoparticles.[7] In addition to the observation of NTE, the experimental Pt L_3 XAS of the clusters is redshifted, and the white line intensity for the He-treated clusters increases with increasing temperature both in H_2 and He atmospheres.[5] Separate XAS calculations were carried out for each Pt atom in nanoclusters generated by 32 randomly chosen configurations sampled from the MD trajectory. To check that this was adequate, we verified that the results changed little from those with 24 configurations and that the leading moments of the Pt-Pt PDFs for 32 configurations agreed with those for the full time series to three significant digits (Fig. 3). Our XAS calculations included all atoms within a radius of 7 Å, i.e., about 150 atoms from the center of the cluster, and used a fully screened core hole and the default Hedin-Lundqvist plasmon-pole self-energy. These calculations used no adjustable parameters; the absolute energy scale was calibrated against that in bulk Pt and the edge positions at each temperature reflect a configurational average of the Fermi energies. Due to the large structure and bonding fluctuations, the results for individual configurations (Fig. 3) show considerable variation. For such cases it is usually not reliable to calculate the XAS in terms of the mean structure and Gaussian Debye-Waller factors, and hence, configurational averaging was necessary.[10] The agreement between our XAS simulations and experiment is remarkable, reproducing all features with the exception of the notable drop in intensity after the white line at high temperature. Given the sensitivity of the XAS to structure, this agreement lends support to the validity and interpretation of our simulations.

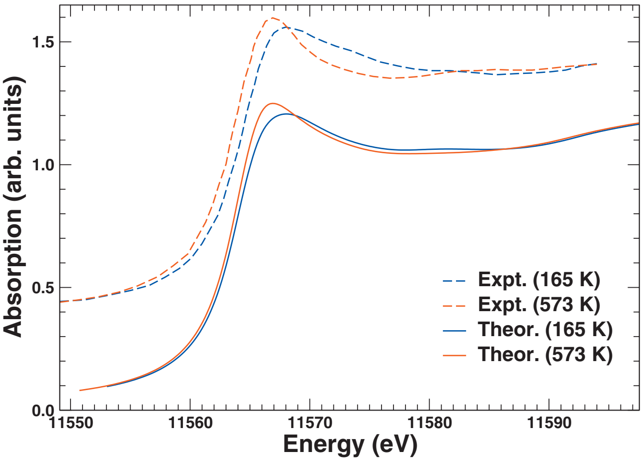

FIG. 3. (Color) Comparison of theoretical (bottom curves) and experimental (top curves shifted for clarity) x-ray absorption near-edge structure (XANES). The theoretical spectra are obtained from a configurational average of 32 random conformations extracted from the last 5.5 ps of the MD simulation. The error bars on the theoretical calculations indicate the standard deviation of fluctuations between the various configurations.

It is also interesting to analyze these results in terms of their electronic structure. Both our DFT and XAS simulations show that the mean Fermi energy (and hence the threshold energy) decreases with increasing temperature with changes of a few tenths of an electron volt,[10] roughly comparable with the observed 0.6 eV redshift in the experimental XAS for the 5–25 atom distribution. Interestingly, the mean charge per Pt atom obtained from a Bader analysis shows significant, temperature-dependent differences between the two populations of Pt atoms. At low (high) temperature the oxidized Pt atoms have an average positive net charge of $+0.23e$ ($+0.27e$) while the metallic ones are slightly negative with $-0.05e$ ($-0.06e$). Thus the observed variation in edge positions with temperature can be attributed to an interplay between charging, chemical shifts, and entropic effects, all driven by the large dynamical fluctuations of the system.

In summary, we have applied a combination of theory and experiment to elucidate the behavior of supported Pt nanoclusters. Our DFT/MD approach addresses the nature of nonequilibrium structure at the nanoscale from a simulated real-time point of view and is a generalization of the conventional treatment in terms of small vibrations about quasiequilibrium positions. Remarkably, our simulations explain many of the unusual properties of these systems, including NTE, anomalous disorder, and thermal variations in electronic structure. A notable revelation is that the disorder is due to large, dynamical fluctuations driven by librational motion and internal flexing. Because of the analogy to hindered Brownian motion, such motion is expected to be a general feature of tethered nanoparticles. Our DFT/MD calculations also explain fluctuating cluster-substrate interactions and charge transfer, consistent with observed variation of the absorption threshold. Finally, these results imply that a real-time DFT/MD approach that accounts for librational motion and fluctuating bonding may be key to a better understanding of the catalytic activity in Pt/γ-Al_2O_3 systems since they point to an enhanced phase space of possible reaction sites and variable electronic structure. Thus because of the close connection between structure, both atomic and electronic, and function, we argue that this dynamic structure picture could lead to a fundamentally new level of understanding of nanoscale materials with potentially important implications for their catalytic properties.

This work is supported by DOE Grants No. DE-FG02-04ER1599 (F.V. and J.J.R.), No. DE-FG03-97ER45623 (J.J.R.), and No. DE-FG02-03ER15476 (R.G.N. and A.I.F.), and NIH NCRR BTP Grant No. RR-01209 (J.K.), and by DOE computer support at NERSC.

---

*Corresponding author. jjr@phys.washington.edu

[1] F. Baletto and R. Ferrando, Rev. Mod. Phys. **77**, 371 (2005).

[2] J. Guzman and B. C. Gates, J. Am. Chem. Soc. **126**, 2672 (2004).

[3] M. Oudenhuijzen, J. A. van Bokhoven, J. T. Miller, D. E. Ramaker, and D. C. Konigsberger, J. Am. Chem. Soc. **127**, 1530 (2005).

[4] H. Haberland, *Clusters of Atoms and Molecules* (Springer-Verlag, New York, 1994).

[5] J. H. Kang, L. D. Menard, R. G. Nuzzo, and A. I. Frenkel, J. Am. Chem. Soc. **128**, 12068 (2006).

[6] L. Menard *et al.*, J. Phys. Chem. B **110**, 14564 (2006).

[7] S. J. L. Billinge and I. Levin, Science **316**, 561 (2007).

[8] R. Car and M. Parrinello, Phys. Rev. Lett. **55**, 2471 (1985).

[9] J. S. Tse, Annu. Rev. Phys. Chem. **53**, 249 (2002).

[10] See EPAPS Document No. E-PRBMDO-78-R08836 for supplementary video clips, figures, and tables. For more information on EPAPS, see http://www.aip.org/pubservs/epaps.html

[11] F. Dzegilenko and E. Herbst, J. Chem. Phys. **100**, 9205 (1994).

[12] Y. V. Roberts, B. F. G. Johnson, and R. E. Benfield, Inorg. Chim. Acta **229**, 221 (1995).

[13] Z. Y. Li, N. P. Young, M. D. Vece, S. Palomba, R. E. Palmer, A. L. Bleloch, B. C. Curley, R. L. Johnston, J. Jiang, and J. Yuan, Nature (London) **451**, 46 (2008).

[14] G. Kresse and J. Furthmüller, Phys. Rev. B **54**, 11169 (1996).

[15] A. L. Ankudinov, B. Ravel, J. J. Rehr, and S. D. Conradson, Phys. Rev. B **58**, 7565 (1998).

[16] A. L. Ankudinov, C. E. Bouldin, J. J. Rehr, J. Sims, and H. Hung, Phys. Rev. B **65**, 104107 (2002).

[17] A. L. Ankudinov, J. J. Rehr, J. J. Low, and S. R. Bare, Top. Catal. **18**, 3 (2002).

[18] J. P. Perdew, K. Burke, and M. Ernzerhof, Phys. Rev. Lett. **77**, 3865 (1996).

[19] L. Wang and D. D. Johnson, J. Am. Chem. Soc. **129**, 3658 (2007).

[20] T. Yokoyama, T. Satsukawa, and T. Ohta, Jpn. J. Appl. Phys., Part 1 **28**, 1905 (1989).

[21] A. I. Frenkel and J. J. Rehr, Phys. Rev. B **48**, 585 (1993).

[22] N. Van Hung and J. J. Rehr, Phys. Rev. B **56**, 43 (1997).

[23] V. F. Petrenko and R. W. Withworth, *Physics of Ice* (Oxford University Press, New York, 1999).